Development of Myelination and Cholinergic Innervation in the Central Auditory System of a Prosimian Primate (*Otolemur garnetti*)

Daniel J. Miller,[1]* Elizabeth P. Lackey,[1] Troy A. Hackett,[2] and Jon H. Kaas[1]

[1]Department of Psychology, Vanderbilt University, Nashville, Tennessee 37205
[2]Department of Speech and Hearing Sciences, Vanderbilt University, Nashville, Tennessee 37205

ABSTRACT

Change in the timeline of neurobiological growth is an important source of biological variation, and thus phenotypic evolution. However, no study has to date investigated sensory system development in any of the prosimian primates that are thought to most closely resemble our earliest primate ancestors. Acetylcholine (ACh) is a neurotransmitter critical to normal brain function by regulating synaptic plasticity associated with attention and learning. Myelination is an important structural component of the brain because it facilitates rapid neuronal communication. In this work we investigated the expression of acetylcholinesterase (AChE) and the density of myelinated axons throughout postnatal development in the inferior colliculus (IC), medial geniculate complex (MGC), and auditory cortex (auditory core, belt, and parabelt) in Garnett's greater galago (*Otolemur garnetti*). We found that the IC and MGC exhibit relatively high myelinated fiber length density (MFLD) values at birth and attain adult-like values by the species-typical age at weaning. In contrast, neocortical auditory fields are relatively unmyelinated at birth and only attain adult-like MFLD values by the species-typical age at puberty. Analysis of AChE expression indicated that, in contrast to evidence from rodent samples, the adult-like distribution of AChE in the core area of auditory cortex, dense bands in layers I, IIIb/IV, and Vb/VI, is present at birth. These data indicate the differential developmental trajectory of central auditory system structures and demonstrate the early onset of adult-like AChE expression in primary auditory cortex in *O. garnetti*, suggesting the auditory system is more developed at birth in primates compared to rodents. J. Comp. Neurol. 521:3804–3816, 2013.

INDEXING TERMS: comparative anatomy; ontogeny; myelin; acetylcholine; neocortex

Comparative studies of ontogeny indicate that primates differ from other mammals in a number of the growth processes that have led to the relative encephalization of primates in general, and humans in particular (Deacon, 1997). These studies indicate that the onset, duration, and rate of change in a particular growth process are critical determinants of the adult phenotype (Bogin, 1999). For example, many primate species develop relatively large brains by modifying the rate of brain growth, and humans generate such large brains by extending the fetal rate of neural growth through the first year of postnatal life (Leigh, 2004; Sakai et al., 2012). In addition, the organization of the basal forebrain nuclei, which produce acetylcholine (ACh), differentiates in parallel with growth of the cerebral cortex and is the most complex in primates and cetaceans (Raghanti et al., 2011; Semba, 2004). Although the exact consequences of differential growth in neurobiological tissues are unclear, these observations suggest that modifications to the developmental schedule of brain growth play a critical role in the evolution of primate cognition.

Prosimian primates represent a major evolutionary branch of the primate radiation, and galagos are one of only a few prosimians available for study. Furthermore, there are no previous studies investigating the development of any sensory system in prosimians.

Grant sponsor: NIH/NIDCD; Grant numbers: RO1 DC04318 (to T.A.H.); N516446 (to J.H.K.).

Corresponding Author: Daniel J. Miller, 111 21st Ave. South, Nashville TN, 37205. E-mail: daniel.j.miller@vanderbilt.edu.

Received February 11, 2013; Revised May 22, 2013;
Accepted May 23, 2013.
DOI 10.1002/cne.23379
Published online June 8, 2013 in Wiley Online Library (wileyonlinelibrary.com)

The prosimian nervous system is thought to be less changed from our early primate ancestors than that of other extant primates, representing the best opportunity to study the neurobiological overlap between primates and commonly used mammalian species, such as rodents (Kaas, 2012). Results from studies of the developing nervous system in galagos therefore apply broadly to other primate taxa and provide insight into the mechanisms at work in the evolution of primate development.

The inferior colliculus (IC) receives input from brainstem nuclei, providing the sole source of subcortical auditory input to the medial geniculate complex (MGC). The MGC, in turn, provides the sole source of auditory input to cortex. In cortex, the core areas (A1 and R) are considered primary regions because they receive the most dense projections from subdivisions of the MGC, specifically the ventral nucleus (MGv), and project heavily to the bordering belt and parabelt regions. The auditory belt and parabelt areas are generally considered successive, higher stages of auditory integration because of dense input from the core areas, and input from the dorsal (MGd) and medial (MGm) nuclei of the MGC (Morel and Kaas, 1992; Morel et al., 1993; Hackett et al., 1998, 2001). The structures of interest in the current worth therefore represent serial stages of neuronal activity along the auditory pathway, such that each synapse informs the receptive field properties that define successive neuronal populations, ultimately determining auditory behavior.

Excitatory neurons in sensory systems of the forebrain generally express molecules that determine synaptic connectivity for a finite period of time during early life, also known as critical periods of development. These critical periods reflect the dynamic interaction between intrinsic and extrinsic processes ultimately responsible for the development of adaptive neural circuitry. ACh is a neurotransmitter associated with synapse formation and activity-dependent plasticity (Lucas-Meunier et al., 2003). Specifically, the cholinergic system modulates the spontaneous firing rate of pyramidal neurons and influences the process of long-term depression and potentiation (Foehring and Lorenzon, 1999; Li, 2012). ACh has also been implicated in Alzheimer's disease and may be important in maintaining synaptic plasticity during adulthood (Bartus et al., 1982; Davies and Maloney, 1976; Descarries et al., 2005). Despite this crucial role, ontogenetic data on the cholinergic system during primate evolution are limited.

In the central nervous system, oligodendrocytes generate myelin, a lipid membrane crucial to normal neurological function in vertebrates. Mammalian forebrain sensory systems exhibit a period of myelination that generally begins during gestation and continues during postnatal life until maturity (Davison and Dobbing, 1966; Moore, 1985). Myelin biogenesis results from a dynamic process of cellular signaling that draws upon the molecular cascades initiated by neuronal activity to promote saltatory action potential conduction, dramatically increasing the speed of neuronal communication (Fields, 2010; Ishibashi et al., 2006; Simons and Trajkovic, 2006; Stevens et al., 2002; Wake et al., 2011). Myelination is thus an important factor in establishing connectivity in the developing brain and facilitates the rapid transfer of information in neural systems.

The present study is the first to investigate the postnatal development of the auditory system in any prosimian primate. We determined the expression level of ACh (measured by acetylcholinesterase [AChE]) and the myelinated fiber length density (MFLD) of axons in the central nucleus of the inferior colliculus (ICc), the dorsal and ventral nuclei of the medial geniculate complex, and the core, medial belt (MB), lateral belt (LB), and parabelt (PB) regions of auditory cortex in galagos ranging in age from newborn to adult. As higher levels of the auditory system depend upon the preceding level(s), myelination patterns are expected to mature subcortically first, and then in the core areas followed by the belt and parabelt regions. In contrast, AChE levels may reflect periods of development when neurons are most subject to changing synaptic contacts. Understanding the time course of myelination and AChE expression of auditory structures in galagos will thus indicate the relative degree of plasticity these structures may exhibit, and when they become fully functional.

MATERIALS AND METHODS

Sample

All procedures involving animals followed the National Institutes of Health (NIH) Guidelines for the Use of Laboratory Animals, and were approved in advance by the Vanderbilt University Institutional Animal Care and Use Committee. Animals used in this study were part of an internal, long-term breeding colony under protocols approved by the Vanderbilt University Institutional Animal Care and Use Committee. The study sample consisted of postmortem brain sections from 20 Garnett's greater galagos (*Otolemur garnetti*) ranging in age from birth to adulthood (Table 1).

All animals were injected with a lethal dose of sodium pentobarbital (60 mg/kg or more; Sigma-Aldrich, St. Louis, MO) and perfused intracardially with phosphate-buffered saline (PBS; 0.1 molar, pH 7.4; Sigma-Aldrich). For fixation, 4% paraformaldehyde (Sigma-Aldrich) in PBS and 4% paraformaldehyde in PBS with 10% sucrose solution were delivered in succession. Immediately after perfusion the brains were removed,

TABLE 1.
Specimens Used in This Study

Age	Region	Hemisphere
0 WK	CORTEX	LEFT
0 WK	BS	LEFT
0 WK	CORTEX	LEFT
1 WK	BS	LEFT
2 WK	ALL	LEFT
2 WK	CORTEX	LEFT
4 WK	ALL	LEFT
4 WK	CORTEX	LEFT
8 WK	CORTEX	BILATERAL
8 WK	ALL	BILATERAL
20 WK	CORTEX	BILATERAL
20 WK	ALL	BILATERAL
50 WK	BS	LEFT
54 WK	CORTEX	LEFT
60 WK	CORTEX	LEFT
2.5 YR	ALL	BILATERAL
3 YR	CORTEX	LEFT
9 YR	ALL	LEFT
15 YR	ALL	BILATERAL
21 YR	CORTEX	LEFT

WK, week; YR, year; CORTEX, neocortex; BS, brainstem and thalamus; ALL, neocortex, brainstem and thalamus; LEFT, left hemisphere; BILATERAL, both hemispheres.

separated from the thalamus and brainstem, and cut into blocks. The blocks containing the temporal lobe or brainstem and thalamus were immersed in 30% sucrose in PBS overnight and then cut in a coronal or semicoronal plane (off-coronal type A, perpendicular to the superior temporal plane and midline) at 20 or 40 μm on a freezing microtome. A 1-in-6 series of adjacent sections were processed with thionin for Nissl substance, the Gallyas silver impregnation method to reveal myelinated axon fibers (Gallyas, 1971), and AChE (Geneser-Jensen and Blackstad, 1971). Architectonic analyses were conducted in sections stained to visualize Nissl substance, myelin, and AChE. The locations of regions of interest were identified based on cytoarchitecture, facilitated by the simultaneous availability of multiple stains, and by descriptions provided in previous publications (Morel and Kaas, 1992; Morel et al., 1993; Hackett et al., 1998, 2001).

Stereology

MFLD was quantified by D.J.M. and E.P.L. using a computerized stereology system consisting of a Nikon E80i microscope with a 100× oil immersion objective lens and StereoInvestigator software (MBF Bioscience, Williston, VT). D.J.M. trained E.P.L. and interrater reliability was assessed by means of the intraclass correlation coefficient, revealing a strong agreement between observers (single measures correlation coefficient = 0.783, $P < 0.001$).

Beginning at a random starting point, three myelin-stained sections equidistantly spaced within available tissue were selected for analysis. Therefore, the sections selected for analysis were distributed across 560 μm (40 μm cut × 3 sections × 1-in-6 series). We used adjacent Nissl- and AChE-stained sections to confirm the cytoarchitecture of each region of interest. In the case of cortical areas, we used Nissl-stained sections to locate the white matter / gray matter interface. MFLD was evaluated using the SpaceBalls probe, a 6-μm sampling hemisphere for lineal features combined with a fractionator sampling scheme (Mouton et al., 2002). Fibers were marked where they intersected the outline of the hemispheric probe. Sampling hemispheres were placed in a systematic random fashion every 280 × 280 μm to cover the region of interest with ~30 frames per section (actual mean = 29.4), and mean mounted section thickness was measured every eight sampling locations. The analysis was performed under Koehler illumination at 100× magnification. To obtain MFLD, the total fiber length was divided by the planimetric measurement of the reference volume that was sampled, as calculated by the StereoInvestigator software. We investigated a total of 10,364 sampling locations.

Densitometry

Laminar density profiles for AChE in the core auditory cortex of each age group were generated using code customized for use with ImageJ by Dr. John Smiley (Nathan Kline Institute, Orangeburg, NY). Three AChE-stained sections equidistantly spaced within available tissue were photographed at 2× magnification (72 dpi) and converted to grayscale for densitometric analysis. Density profiles were recorded as transects from the lower boundary of cortical layer VI to the pial surface across core auditory cortex. Adjacent Nissl-stained sections were used to locate the white matter / gray matter interface. DJM recorded a total of 1,637 transects (actual mean per age group = 233.8), each containing an average of 1,106.4 measurements.

Data analysis

Photomicrographs were produced using the Adobe suite software (San Jose, CA). All images were modified up to 5% of their brightness and contrast to match image quality across figures. The R software program was used for statistical analysis. Probability values (P) lower than 0.05 were considered significant.

In the analysis of MFLD data, best-fit curves depicting growth effects during development were calculated using hierarchical multiple regression for linear, quadratic, and cubic functions. Initial groups were determined based on life history stages (for reviews, see Leigh and Park,

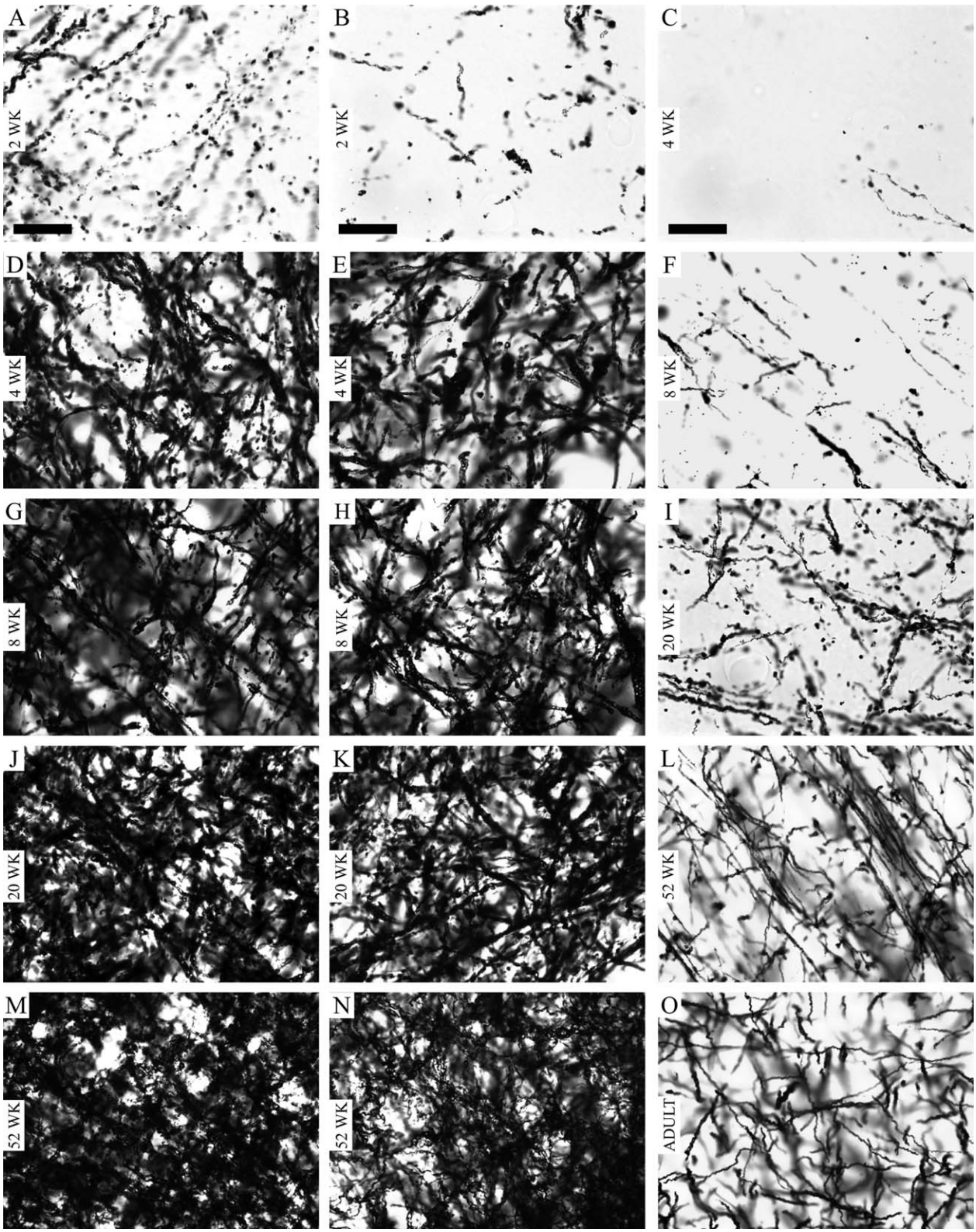

Figure 1. Developmental series of high-magnification photos of the galago auditory system. Representative sections from the central nucleus of the inferior colliculus **(A,D,G,J,M)**, ventral nucleus of the medial geniculate complex **(B,E,H,K,N)** and layer III of primary auditory cerebral cortex **(C,F,I,L,O)** stained for myelinated axons and vertically arranged by age. Weaning occurs at 20 weeks; puberty occurs at 52 weeks. WK, week. Scale bars = 20 μm.

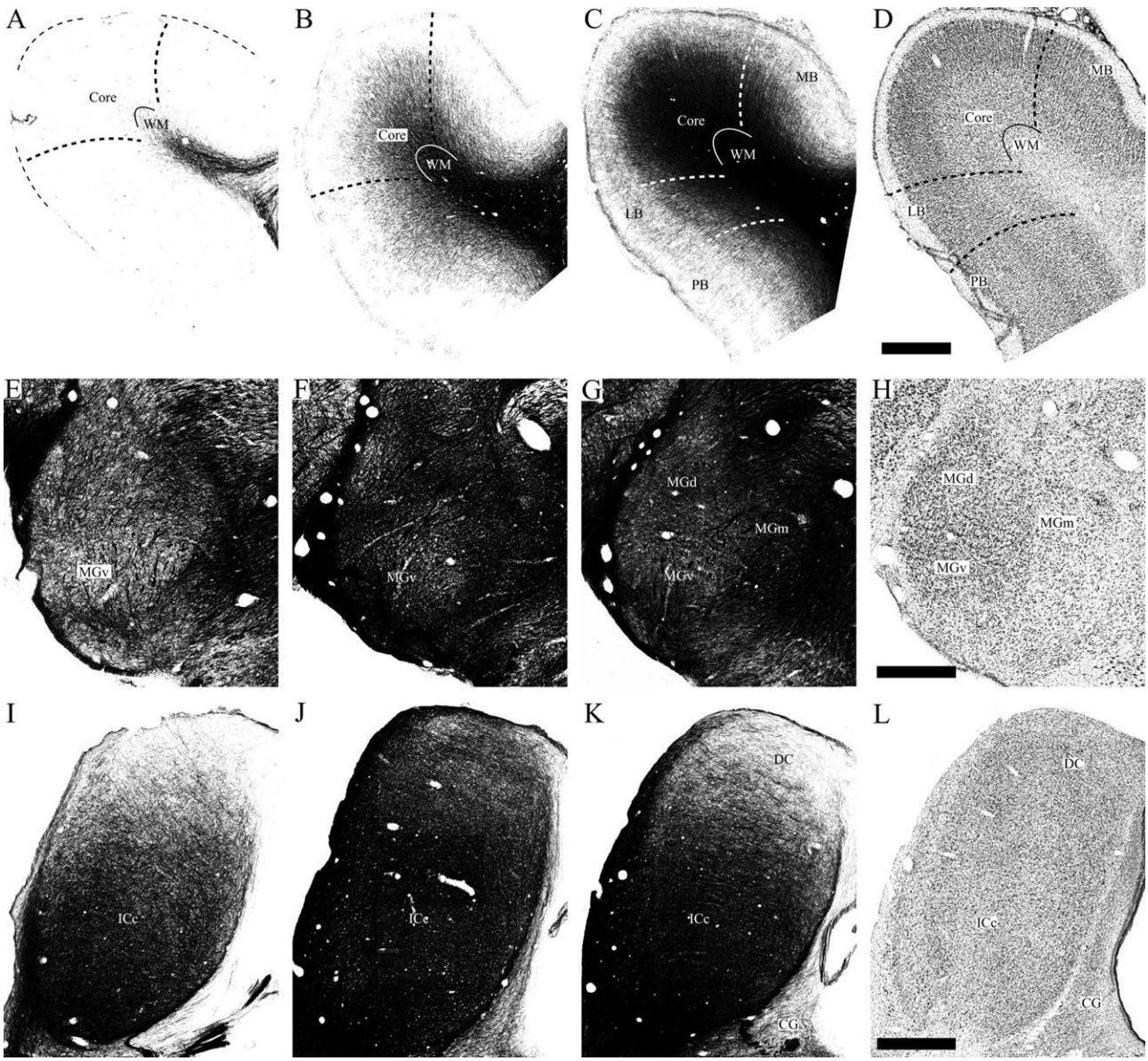

Figure 2. Developmental series of low-magnification photos of galago auditory system. Representative sections from the IC, MGC, and auditory neocortex stained for myelinated axons **(A–C,E–G,I–K)** and neuron cell bodies **(D,H,L)**. Photographs are arranged by region of interest along the vertical axis (Neocortex, A–D; MGC, E–H; IC, I–L) and by age along the horizontal axis (A, 4 weeks; B, 20 weeks; C,D, adult; E,I, 0 weeks; F,J, 20 weeks; G,H,K,L, adult). Dashed lines delineate edges of tissue, and regions of interest. WM, white matter; DC, dorsal cortex of the IC; CG, central gray matter. Scale bars = 1 mm.

1998; Bogin, 1999; Kennedy, 2005), punctuated by the species-typical age at weaning (~20 weeks), and puberty (~52 weeks or 1 year; Ehrlich, 1974). We grouped older adult values together at the first postpubertal age to summarize variability due to senescent processes.

In the analysis of AChE laminar density profiles, transects were normalized to account for interimage variability and divided into 20 bins, each containing an average of 54.7 measurements. Bins were grouped according to their respective layers and the Welch's T statistic was calculated to determine differences in the density of AChE expression. The Welch's T statistic was calculated for density values in each of the following comparisons: layer I < layer II and upper layer III; lower layer III (IIIb) and upper layer IV < layer II, upper layer III, lower layer IV and upper layer V; lower layer V (Vb) and upper layer VI < lower layer IV, upper layer V and lower layer VI.

RESULTS

All of the regions in our cross-sectional sample (Table 1) showed increasing myelination with age (Figs. 1, 2).

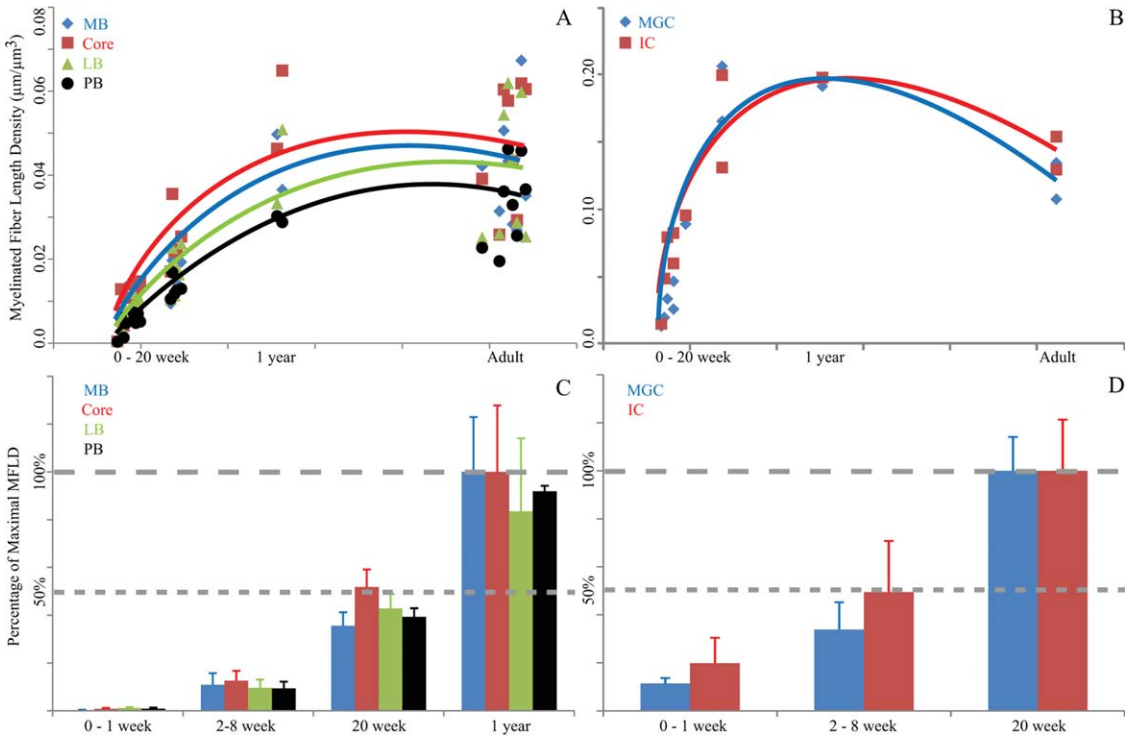

Figure 3. Developmental trajectory of MFLD. Graphs show best-fit curves and percent adult fiber density values for MFLD in galagos (n = 20) for neocortical **(A,C)** and subcortical structures **(B,D)**. MFLD values are plotted along the vertical axis. The horizontal axis is arranged by postnatal age (A,B). Percent maximal density values are plotted along the vertical axis, the short dashed line represents 50% maximal values and the long dashed line represents 100% maximal values (C,D). A: Diamonds represent the MB, squares represent the core, triangles represent the LB, and circles represent the PB regions of auditory neocortex. B: Diamonds represent the MGC, squares represent the IC. C: Blue represents the MB, red represents the core, gold represents the LB, and black represents the PB. D: Blue represents the MGC, red represents the IC.

The stereological quantification of myelin in our sample produced data best fit by a quadratic growth curve (Fig. 3, Table 2; see Materials and Methods). The ICc and the MGv and MGd of the thalamus achieved maximal fiber density values at earlier life-history periods than cortical auditory fields (Fig. 3; Table 3). All of the age groups in our sample showed statistically significantly more dense AChE staining in layers I, IIIb/IV, and Vb/VI compared to surrounding layers (Figs. 4, 5, Table 4).

The length density of myelinated axons in cortical gray matter at birth is extremely low (~0.0004 $\mu m/\mu m^3$), but increases rapidly thereafter until sexual maturity (Figs. 1, 2). Specifically, mean cortical MFLD at birth is ~1% of the maximal values attained in our sample, but achieves ~46% of the maximal values by the end of weaning (~20 weeks) and approximates maximal adult-like values by puberty (~1 year; Ehrlich, 1974) (Fig. 3; Table 3). The developmental trajectory of cortical MFLD in our sample was best fit by a quadratic regression function for all regions (Fig. 3; Table 2). The core auditory areas exhibited the highest neocortical gray matter myelinated fiber density values throughout life, and the PB had the lowest average values (Fig. 3; Table 3). Qualitative observation of cortical auditory fields identified a rostral to caudal gradient of increasing myelination that was present throughout life in galagos (Fig. 6).

In contrast to the neocortex, subcortical MFLD values observed at birth are relatively high (>0.01 $\mu m/\mu m^3$) and increase until the species-typical age at weaning (Fig. 3). Specifically, neonatal MFLD in the IC and MGC is 19.9% and 11.5%, respectively, of the maximal values in our sample, and both regions attain maximal density around 20 weeks after birth (Figs. 1–3; Table 3). The developmental trajectory of MFLD in the IC and MGC was best fit by a quadratic regression function (Fig. 3; Table 2).

Staining for AChE in the IC was diffuse throughout life, and the dorsal cortex (DC) stains more heavily than the ICc (Fig. 4). From birth onward, AChE expression in the MGC revealed more dense staining of the MGv and MGd compared to the MGm (Fig. 4). Staining for AChE in the core area of auditory cortex revealed that the adult-like distribution of AChE was present at birth (Figs. 4, 5). Specifically, staining in the core auditory field revealed dense bands of AChE in the molecular (I),

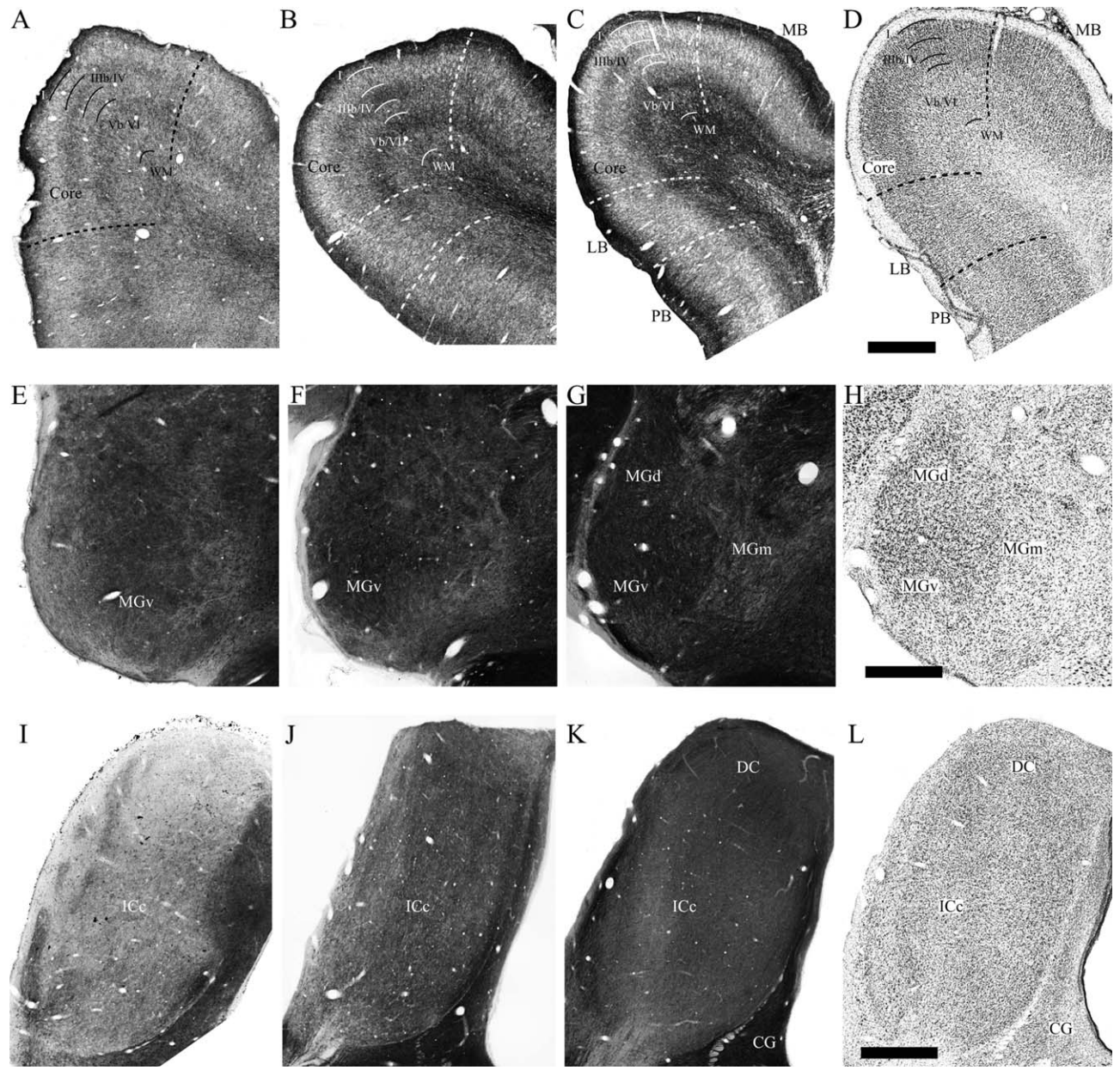

Figure 4. Developmental series of low-magnification photos of AChE expression in galago auditory system. Representative sections from the auditory neocortex **(A–D)**, MGC **(E–H)** and IC **(I–L)** stained for AChE (A–C, E–G, I–K) and neuronal cell bodies (D,H,L). Photographs are arranged by region of interest along the vertical axis and by age along the horizontal axis (A,E,I, 0 weeks; B,F,J, 20 weeks; C,D,G,H,K,L, adult). I, molecular layer 1; IIIb/IV, granular layers 3b/4; Vb/VI, infragranular layers 5b/6; WM, white matter. Scale bars = 1 mm.

granular (IIIb/IV), and infragranular layers (Vb/VI) (Figs. 4, 5; Table 4). In addition, the infragranular layers near the white matter / gray matter interface showed an overall increase in staining density after the first 4 weeks of postnatal life (H_0: age $<$ 4 weeks vs. age $>$ 4 weeks; Welch's T statistic, 40.65; $P = 0.00001$)

DISCUSSION

Our data demonstrate the differential developmental trajectory of structures in the central auditory system and distinguish the immediate postnatal expression of AChE in auditory cortex of Garnett's greater galago from that of other mammals, such as rodents. Auditory fields in the cerebral cortex of this prosimian primate exhibit fewer myelinated axons at birth and attain mature density values later than subcortical auditory structures. Our sample of prosimian auditory cortex conforms to the typical primate pattern of laminar AChE expression (Morel and Kaas, 1992; Morel et al., 1993; Hackett et al., 1998, 2001), differing from other mammals such as rodents in that the adult-like pattern of AChE immunoreactivity is

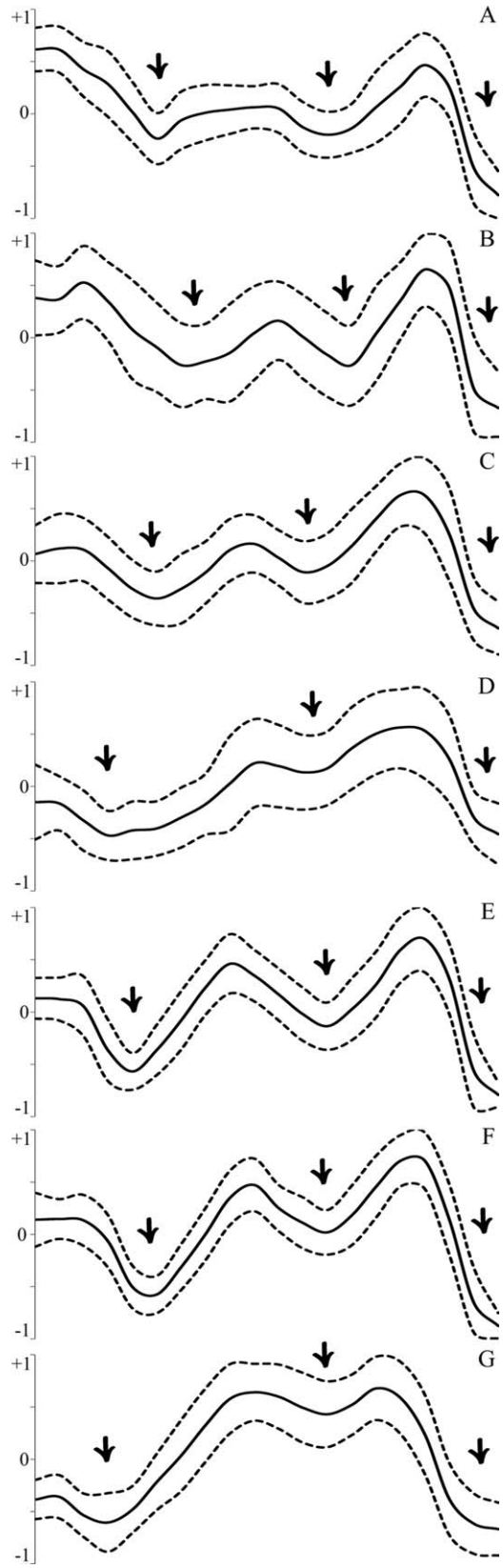

Figure 5.

present at birth (Hohmann and Ebner, 1985; Robertson et al., 1991; Semba, 2004; Shideler and Yan, 2010). Early life-history stages are periods of intense learning in primates as the trend towards increasing lifespan and sophisticated social behavior places selective pressure on the convergence of neurobiological growth processes and exposure to novel social and environmental factors. Therefore, modification to the developmental schedule of neurobiological connectivity in the auditory system during primate evolution may contribute to the neurobiological substrates of adaptive auditory-related behaviors, perhaps as a result of differential plasticity during critical periods in development.

ACh is a major nervous system neurotransmitter and the cortical branch of the cholinergic system is primarily innervated by the basal forebrain nuclei, or the nucleus of Meynert in primates (Semba, 2004; Raghanti et al., 2011). Early studies of the cholinergic system in a wide range of species identified a positive correlation between the size and organization of cholinergic nuclei and the evolution of the cerebral cortex such that the cholinergic nuclei of the basal forebrain differentiate as cortical volume increases (Gorry, 1963). Studies of the cholinergic system have employed a variety of techniques to infer the presence and localization of ACh, making it difficult to draw firm conclusions. Despite this difficulty, the onset of cholinergic activity seems to occur during gestation in mammals (Nadler et al., 1973; Coyle and Yamamura, 1976; Kostovic and Goldman-Rakic, 1983; Krmpotic-Nemanic et al., 1983; Hohman et al., 1985; Heckers et al., 1992), and the volume of cholinergic nuclei increased during mammalian evolution (Gorry, 1963; Semba, 2004; Raghanti et al., 2011). Cholinergic innervation of the cerebral cortex in rodents appears shortly after birth and enzymatic activity associated with ACh increases to adult levels and exhibits the mature laminar distribution by the end of the third postnatal week, around the time of the species-typical transition into adulthood (Coyle and Yamamura, 1976; Hohmann and

Figure 5. Developmental series of AChE laminar density profiles in core auditory cortex. Graphs show laminar density profiles of AChE expression in the core area of auditory cortex from each age group (**A,** 0 weeks; **B,** 2 weeks; **C,** 4 weeks; **D,** 8 weeks; **E,** 20 weeks; **F,** 52 weeks; **G,** adult). Data are represented as normalized density values that vary along the y-axis between −1 (dense staining) and +1 (light staining). Data are represented along the x-axis as transects across the cortical layers, such that layer VI is represented on the left and layer I is represented on the right. Arrows depict cortical layers Vb/VI (left), IIIb/IV (middle), and I (right) tested for increased AChE staining using Welch's T statistic (see Materials and Methods and Table 4). The solid line represents the mean laminar density profile and the dashed lines represent the standard deviation from the mean.

TABLE 2.
Best-fit Regression Functions for MFLD Data

Region	Function	Adj. R^2	*P* value
IC	Quadratic	0.8318	0.00028
MGC	Quadratic	0.8966	0.00002
MB	Quadratic	0.7491	0.00182
Core	Quadratic	0.7668	0.00011
LB	Quadratic	0.6929	0.00317
PB	Quadratic	0.8048	0.00260

Values calculated by using hierarchical multiple regression analysis with adults as endpoint (see Materials and Methods).

Ebner, 1985; Aubert et al., 1996). Our data provide evidence that the distribution of AChE in the core auditory area in Garnett's greater galago at birth is more adult-like than would be expected based on previous work in rodents and other mammals. However, this prosimian primate is similar to rodents in that the intensity of AChE expression in the infragranular layers of the cortical mantle near the white matter / gray matter interface tends to increase during the first month of postnatal life. Our results suggest that the distinct pattern of AChE expression in higher-order structures of the prosimian auditory system compared to other mammals may be important in the evolution of complex auditory behavior in primates.

Myelination is ubiquitous throughout the vertebrate nervous system and critical to normal neurological function, playing an important role in neuronal communication by regulating axon conductance and resistivity (Waxman, 1977; Simons and Trotter, 2007). The myelin sheath is also important from functional and engineering standpoints because it permits an order of magnitude faster conduction velocity with a minimal volumetric cost (Waxman, 1977). The density of myelinated axons is a common metric in basic descriptive work of cortical field identity (Krubitzer and Kaas, 1990; Preuss and Goldman-Rakic, 1991; Bock et al., 2011) and has been used to assess the relative maturity of brain regions (Flechsig, 1901; Langworthy, 1933; Yakovlev and Lecours, 1967; Gibson, 1970; Moore et al., 1995; Moore and Linthicum, 2001; Miller et al., 2012). However, methodological heterogeneity among previous histological studies of myelination has made direct comparisons between regions or species difficult (Langworthy, 1933; Yakovlev and Lecours, 1967; Gibson, 1970; Moore, 1985; Brody et al., 1987; Kinney et al., 1988; Benes, 1989; Moore et al., 1995, 1996, 1997; Moore and Guan, 2001; Moore and Linthicum, 2001; Abraham et al., 2010; Takahashi et al., 2011; Miller et al., 2012). Despite differences in the timing of the onset of myelination in different species and of specific fiber tracts, mammalian forebrain sensory system myelination is generally complete by puberty, if not before (Langworthy, 1933; Davison and Dobbing, 1966; Gilles, 1976; Moore, 1985; Looney and Elberger, 1986; Moore et al., 1995; Moore and Linthicum, 2001; Levitt, 2003; Watson et al., 2006). Work in rodents, for example, has

TABLE 3.
Percent of Maximal, Mature Adult MFLD During Different Developmental Stages in Auditory System

		Neonate		Weaning	Puberty
		0 - 1 WK	2 - 8 WK	20 WK	1 YR
IC	Mean	19.9 (2)	49.5 (3)	MAX (1)	MAX
	SEM	*10.5*	*5.3*	*21.3*	*NA*
MGC	Mean	11.5 (2)	33.9 (3)	MAX (1)	MAX
	SEM	*2.2*	*11.3*	*14.1*	*NA*
MB	Mean	0.2 (2)	19.9 (8)	36.5 (2)	MAX (2)
	SEM	*0.3*	*4.8*	*5.6*	*22.9*
Core	Mean	0.3 (2)	21.2 (8)	51.7 (2)	MAX (2)
	SEM	*0.4*	*4.1*	*7.3*	*27.8*
LB	Mean	0.2 (2)	17.3 (8)	41.9 (2)	MAX (2)
	SEM	*0.3*	*3.5*	*6.1*	*30.5*
PB	Mean	0.3 (2)	13.8 (8)	38.8 (2)	88.9 (2)
	SEM	*0.4*	*2.8*	*3.6*	*2.3*

MFLD values arranged by life history and age, divided by maximum adult density; all values represent percentages. Parentheses indicate number of specimens in calculation. WK, week; YR, year; SEM, standard error of the mean; MAX, maximal adult value; NA, not applicable due to sample size.

TABLE 4.
Statistical Tests on Differences Between Average Laminar AChE Density

Age group	Layer	Welch's T	*P* value
0 WK	I	37.09	0.00002
	IIIb/IV	11.04	0.00079
	Vb/VI	27.31	0.00005
2 WK	I	36.66	0.00002
	IIIb/IV	9.82	0.00111
	Vb/VI	26.98	0.00005
4 WK	I	59.04	0.00005
	IIIb/IV	10.81	0.00084
	Vb/VI	24.92	0.00007
8 WK	I	64.41	0.00004
	IIIb/IV	10.03	0.00105
	Vb/VI	20.91	0.00012
20 WK	I	41.61	0.00001
	IIIb/IV	15.38	0.00029
	Vb/VI	19.45	0.00015
1 YR	I	55.98	0.00006
	IIIb/IV	12.01	0.00062
	Vb/VI	23.57	0.00008
Adult	I	80.53	0.00002
	IIIb/IV	7.12	0.00284
	Vb/VI	12.11	0.00061

Welch's T statistic and the associated *P* values for the three comparisons among cortical layers in each age group (see Materials and Methods). Layer I was compared to layer II and upper layer III. Lower layer III (IIIb) and upper layer IV were compared to layer II, upper layer III, lower layer IV and upper layer V. Lower layer V (Vb) and upper layer VI were compared to lower layer IV, upper layer V and lower layer VI. *P* values lower than 0.05 were considered significant. WK, week; YR, year.

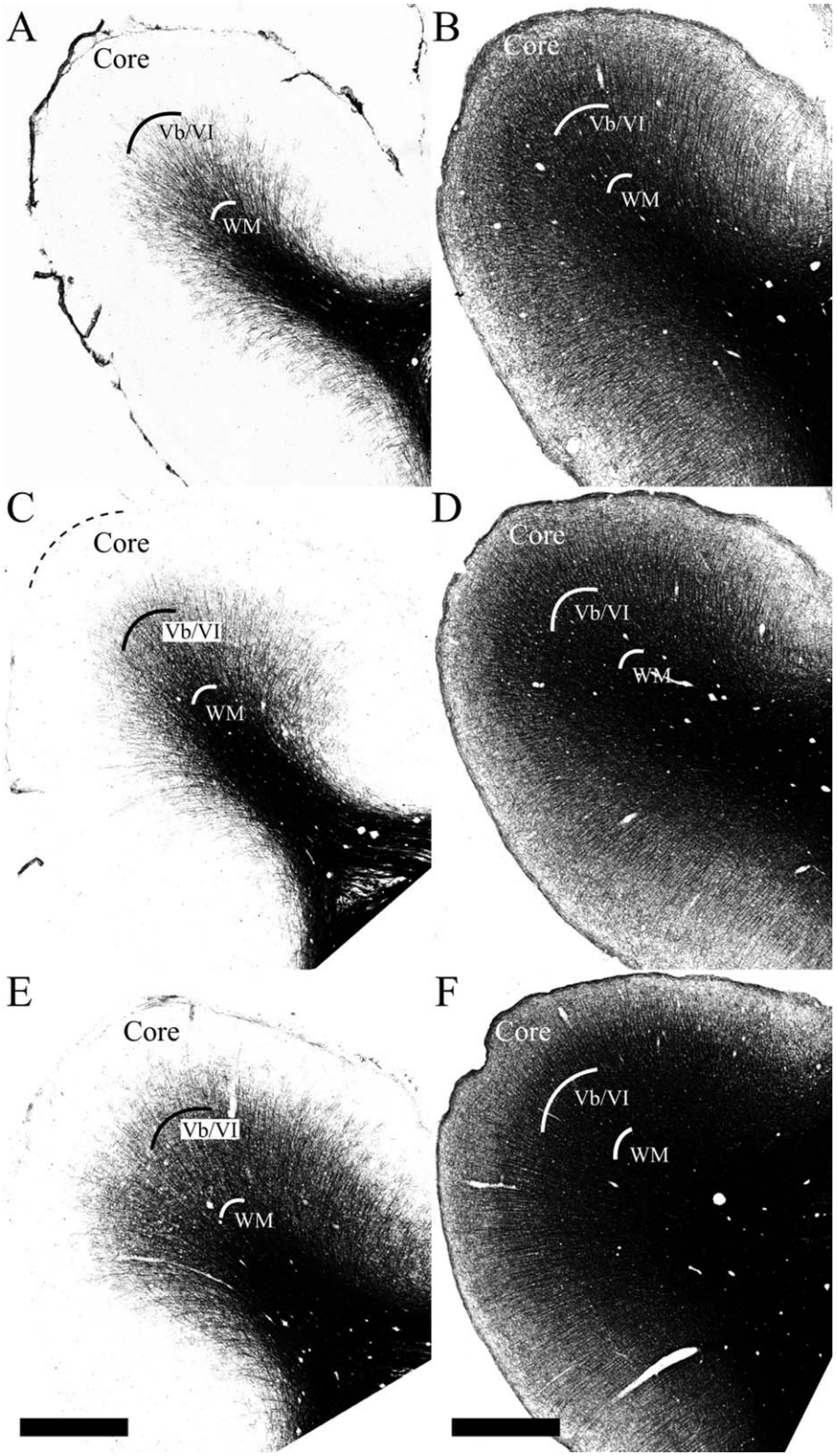

Figure 6. Rostral to caudal gradient of increasing myelination density during development and adulthood. Representative sections from the rostral (upper) to caudal (lower) temporal lobe of the core auditory area of the cerebral cortex in galagos stained for myelin. The horizontal axis is arranged by age (8 weeks, **A,C,E;** adult, **B,D,F**), and the vertical axis is arranged by position along the temporal lobe. Dashed line in C marks outer edge of section. WM, white matter. Scale bar = 1 mm.

shown that myelination of the corpus callosum and internal capsule is complete by the transition between weaning and adulthood (Hamano et al., 1996, 1998), coincident with an age-related decrease in the expression of myelin-related genes in rats (Matsuoka et al., 2010), and that mice exhibit a critical period of myelination that ends around the onset of fertility (Makinodan et al., 2012). Previous nonhuman primate research indicates that neocortical myelination is also complete by the onset of full reproductive maturity in macaque monkeys and chimpanzees (Gibson, 1970; Knickmeyer et al., 2010; Miller et al., 2012). In contrast to these results, myelination in humans continues well into adulthood (Yakovlev and Lecours, 1967; Sowell et al., 2003; Miller et al., 2012). Using stereologic methods to quantify the length density of myelinated axon fibers within the gray matter of the cerebral cortex and subcortical nuclei, our data corroborate previous observations based on histological and neuroimaging techniques that cortical myelination proceeds in a caudal to rostral gradient, that myelin develops in primary before secondary cortical areas, and that subcortical areas mature earlier than neocortical regions in mammals (Flechsig, 1901; Langworthy, 1933; Davison and Dobbing, 1966; Yakovlev and Lecours, 1967; Gibson, 1970; Moore, 1985; Brody et al., 1987; Kinney et al., 1988; Benes, 1989; Moore et al., 1995, 1996, Moore and Guan, 2001; 1997; Gogtay et al., 2004; Moore and Linthicum, 2007; Sano et al., 2007, 2008; Knickmeyer et al., 2008, 2010; Shaw et al., 2008; Deoni et al., 2011; Miller et al., 2012; Shi et al., 2013). Specifically, our data indicate that myelination of subcortical auditory structures such as the MGC and IC attain fully mature fiber density profiles at weaning, a full life-history stage before the cortical auditory fields which attain maximal density values around puberty. These data provide evidence that the ancestral mammalian trend to complete myelination at or before puberty is conserved in prosimian primates. Furthermore, these results are consistent with the conclusion that the auditory pathway is a hierarchical system and may not be fully functionally developed until the onset of sexual maturity.

The functional significance of the differential expression of AChE in early development of the core auditory cortex in primates is uncertain, in part because AChE may not guarantee the presence of ACh. However, one possibility is that during early development ACh acts as a trophic factor (Ruediger and Bolz, 2007), supporting a specific population of afferent fibers that may contribute to a distinct pattern of laminar innervation in primates compared to other mammals. An alternative possibility is that ACh has a modulatory impact on the release of other neurotransmitters (Metherate and Hsieh, 2003; Semba, 2004) and thus serves to regulate neuronal response properties more globally (Zhang, 2006). Myelination is a relatively late-stage developmental process and recent evidence indicates that myelin growth is stimulated by activity-dependent molecular cascades (Wake et al., 2011). The observation that myelination of the auditory cortex largely takes place after the development of AChE expression suggests that ACh is an important modulatory influence on synaptic activity in early postnatal development and may similarly facilitate myelin growth. Together, these observations suggest that the core auditory cortex in primates may exhibit distinct physiological properties and connections compared to rodents as a result of the laminar-specific expression of ACh at birth. ACh expression is decreased in neurodegenerative diseases like Alzheimer's (Davies and Maloney, 1976; Bartus et al., 1982), and may be important in maintaining specific physiological properties in neurons important in attention, learning, and memory during adulthood (Semba, 2004). Given the observation that humans lose more neocortical tissue during aging than other primates (Sherwood et al., 2011) and that cholinergic nuclei expand in parallel with neocortical tissue (Gorry, 1963), these first observations of sensory system development in any of the prosimian primates are consistent with the conclusion that the adult-like distribution of AChE expression at the time of birth in the core area of auditory cortex in primates is distinct from that in other mammals, and may play an important role in the evolution of primate cognition and auditory behavior.

ACKNOWLEDGMENTS

The authors thank Laura Trice, Suzanne Blumell, and Dr. John Smiley for technical assistance.

CONFLICT OF INTEREST

All authors declare no conflict of interest.

ROLE OF AUTHORS

All authors had access to all the data in the study and take responsibility for the integrity of the data and the accuracy of the data analysis. Study concept and design: DJM, TAH, JHK. Acquisition of data: DJM, EPL. Analysis and interpretation of data: DJM, TAH, JHK. Drafting of the article: DJM, EPL. Critical revision of the article for important intellectual content: DJM, TAH, JHK. Obtained funding: TAH, JHK.

LITERATURE CITED

Abraham H, Vincze A, Jewgenow I, Veszpremi B, Kravjak A, Gomori E, Seress L. 2010. Myelination in the human

hippocampal formation from midgestation to adulthood. Int J Dev Neurosci 28:401–410.
Aubert I, Cecyre D, Gauthier S, Quirion R. 1996. Comparative ontogenic profile of cholinergic markers, including nicotinic and muscarinic receptors, in the rat brain. J Comp Neurol 369:31–55.
Bartus RT, Dean RL 3rd, Beer B, Lippa AS. 1982. The cholinergic hypothesis of geriatric memory dysfunction. Science 217:408–414.
Benes FM. 1989. Myelination of cortical-hippocampal relays during late adolescence. Schizophr Bull 15:585–593.
Bock NA, Hashim E, Kocharyan A, Silva AC. 2011. Visualizing myeloarchitecture with magnetic resonance imaging in primates. Ann N Y Acad Sci 1225–1228.
Bogin B. 1999. Evolutionary perspective on human growth. Annu Rev Anthropol 28:109–153.
Brody BA, Kinney HC, Kloman AS, Gilles FH. 1987. Sequence of central nervous system myelination in human infancy. I. An autopsy study of myelination. J Neuropathol Exp Neurol 46:283–301.
Coyle JT, Yamamura HI. 1976. Neurochemical aspects of the ontogenesis of cholinergic neurons in the rat brain. Brain Res 118:429–440.
Davies P, Maloney AJ. 1976. Selective loss of central cholinergic neurons in Alzheimer's disease. Lancet 2:1403.
Davison AN, Dobbing J. 1966. Myelination as a vulnerable period in brain development. Br Med Bull 22:40–44.
Deacon TW. 1997. What makes the human brain different? Annu Rev Anthropol 26:337–357.
Deoni SC, Mercure E, Blasi A, Gasston D, Thomson A, Johnson M, Williams SC, Murphy DG. 2011. Mapping infant brain myelination with magnetic resonance imaging. J Neurosci 31:784–791.
Descarries L, Aznavour N, Hamel E. 2005. The acetylcholine innervation of cerebral cortex: new data on its normal development and its fate in the hAPP(SW,IND) mouse model of Alzheimer's disease. J Neural Transm 112:149–162.
Ehrlich A. 1974. Infant development in two prosimian species: greater galago and slow loris. Dev Psychobiol 7:439–454.
Fields RD. 2010. Neuroscience. Change in the brain's white matter. Science 330:768–769.
Flechsig P. 1901. Developmental (myelogenetic) localization of the cerebral cortex in the human subject. Lancet 2: 1027–1029.
Foehring RC, Lorenzon NM. 1999. Neuromodulation, development and synaptic plasticity. Can J Exp Psychol 53:45–61.
Gallyas F. 1971. A principle for silver staining of tissue elements by physical development. Acta Morphol Acad Sci Hung 19:57–71.
Geneser-Jensen FA, Blackstad TW. 1971. Distribution of acetyl cholinesterase in the hippocampal region of the guinea pig. I. Entorhinal area, parasubiculum, and presubiculum. Z Zellforsch Mikrosk Anat 114:460–481.
Gibson KR. 1970. Sequence of myelinization in the brain of *Macaca mulatta*. University of California, Berkeley.
Gilles FH. 1976. Myelination in the neonatal brain. Hum Pathol 7:244–248.
Gogtay N, Giedd JN, Lusk L, Hayashi KM, Greenstein D, Vaituzis AC, Nugent TF 3rd, Herman DH, Clasen LS, Toga AW, Rapoport JL, Thompson PM. 2004. Dynamic mapping of human cortical development during childhood through early adulthood. Proc Natl Acad Sci U S A 101: 8174–8179.
Gorry JD. 1963. Studies on the comparative anatomy of the ganglion basale of Meynert. Acta Anat (Basel) 55:51–104.
Hackett TA, Stepniewska I, Kaas JH. 1998. Subdivisions of auditory cortex and ipsilateral cortical connections of the parabelt auditory cortex in macaque monkeys. J Comp Neurol 392:475–495.
Hackett TA, Preuss TM, Kaas JH. 2001. Architectonic identification of the core region in auditory cortex of macaques, chimpanzees and humans. J Comp Neurol 441:197–222.
Hamano K, Iwasaki N, Takeya T, Takita H. 1996. A quantitative analysis of rat central nervous system myelination using the immunohistochemical method for MBP. Brain Res Dev Brain Res 93:18–22.
Hamano K, Takeya T, Iwasaki N, Nakayama J, Ohto T, Okada Y. 1998. A quantitative study of the progress of myelination in the rat central nervous system, using the immunohistochemical method for proteolipid protein. Brain Res Dev Brain Res 108:287–293.
Heckers S, Geula C, Mesulam MM. 1992. Cholinergic innervation of the human thalamus: dual origin and differential nuclear distribution. J Comp Neurol 325:68–82.
Hohmann CF, Ebner FF. 1985. Development of cholinergic markers in mouse forebrain. I. Choline acetyltransferase enzyme activity and acetylcholinesterase histochemistry. Brain Res 355:225–241.
Ishibashi T, Dakin KA, Stevens B, Lee PR, Kozlov SV, Stewart CL, Fields RD. 2006. Astrocytes promote myelination in response to electrical impulses. Neuron 49:823–832.
Kaas JH. 2012. The evolution of neocortex in primates. Prog Brain Res 195:91–102.
Kennedy GE. 2005. From the ape's dilemma to the weanling's dilemma: early weaning and its evolutionary context. J Hum Evol 48:123–145.
Kinney HC, Brody BA, Kloman AS, Gilles FH. 1988. Sequence of central nervous system myelination in human infancy. II. Patterns of myelination in autopsied infants. J Neuropathol Exp Neurol 47:217–234.
Knickmeyer RC, Gouttard S, Kang C, Evans D, Wilber K, Smith JK, Hamer RM, Lin W, Gerig G, Gilmore JH. 2008. A structural MRI study of human brain development from birth to 2 years. J Neurosci 28:12176–12182.
Knickmeyer RC, Styner M, Short SJ, Lubach GR, Kang C, Hamer R, Coe CL, Gilmore JH. 2010. Maturational trajectories of cortical brain development through the pubertal transition: unique species and sex differences in the monkey revealed through structural magnetic resonance imaging. Cereb Cortex 20:1053–1063.
Kostovic I, Goldman-Rakic PS. 1983. Transient cholinesterase staining in the mediodorsal nucleus of the thalamus and its connections in the developing human and monkey brain. J Comp Neurol 219:431–447.
Krmpotic-Nemanic J, Kostovic I, Kelovic Z, Nemanic D, Mrzljak L. 1983. Development of the human fetal auditory cortex: growth of afferent fibres. Acta Anat (Basel) 116:69–73.
Krubitzer LA, Kaas JH. 1990. Cortical connections of MT in four species of primates: areal, modular, and retinotopic patterns. Vis Neurosci 5:165–204.
Langworthy OR. 1933. Development of behavior patterns and myelination of the nervous system in the human fetus and infant. In: Contributions to embryology, vol.XXVI. Washington, DC: Carnegie Institute of Washington. p 1–57.
Leigh SR. 2004. Brain growth, life history, and cognition in primate and human evolution. Am J Primatol 62:139–164.
Leigh SR, Park PB. 1998. Evolution of human growth prolongation. Am J Phys Anthropol 107:331–350.
Levitt P. 2003. Structural and functional maturation of the developing primate brain. J Pediatr 143(4 Suppl):S35–45.

Li SC. 2012. Neuromodulation of behavioral and cognitive development across the life span. Dev Psychol 48:810–814.

Looney GA, Elberger AJ. 1986. Myelination of the corpus callosum in the cat: time course, topography, and functional implications. J Comp Neurol 248:336–347.

Lucas-Meunier E, Fossier P, Baux G, Amar M. 2003. Cholinergic modulation of the cortical neuronal network. Pflugers Arch 446:17–29.

Makinodan M, Rosen KM, Ito S, Corfas G. 2012. A critical period for social experience-dependent oligodendrocyte maturation and myelination. Science 337:1357–1360.

Matsuoka T, Sumiyoshi T, Tsunoda M, Takasaki I, Tabuchi Y, Uehara T, Itoh H, Suzuki M, Kurachi M. 2010. Change in the expression of myelination/oligodendrocyte-related genes during puberty in the rat brain. J Neural Transm 117:1265–1268.

Metherate R, Hsieh CY. 2003. Regulation of glutamate synapses by nicotinic acetylcholine receptors in auditory cortex. Neurobiol Learn Mem 80:285–290.

Miller DJ, Duka T, Stimpson CD, Schapiro SJ, Baze WB, McArthur MJ, Fobbs AJ, Sousa AM, Sestan N, Wildman DE, Lipovich L, Kuzawa CW, Hof PR, Sherwood CC. 2012. Prolonged myelination in human neocortical evolution. Proc Natl Acad Sci U S A 109:16480–16485.

Moore DR. 1985. Postnatal development of the mammalian central auditory system and the neural consequences of auditory deprivation. Acta Otolaryngol Suppl 421:19–30.

Moore JK, Guan YL. 2001. Cytoarchitectural and axonal maturation in human auditory cortex. J Assoc Res Otolaryngol 2:297–311.

Moore JK, Linthicum FH Jr. 2007. The human auditory system: a timeline of development. Int J Audiol 46:460–478.

Moore JK, Perazzo LM, Braun A. 1995. Time course of axonal myelination in the human brainstem auditory pathway. Hear Res 87:21–31.

Moore JK, Ponton CW, Eggermont JJ, Wu BJ, Huang JQ. 1996. Perinatal maturation of the auditory brain stem response: changes in path length and conduction velocity. Ear Hear 17:411–418.

Moore JK, Guan YL, Shi SR. 1997. Axogenesis in the human fetal auditory system, demonstrated by neurofilament immunohistochemistry. Anat Embryol (Berl) 195:15–30.

Morel A, Kaas JH. 1992. Subdivisions and connections of auditory cortex in owl monkeys. J Comp Neurol 318:27–63.

Morel A, Garraghty PE, Kaas JH. 1993. Tonotopic organization, architectonic fields, and connections of auditory cortex in macaque monkeys. J Comp Neurol 335:437–459.

Mouton PR, Gokhale AM, Ward NL, West MJ. 2002. Stereological length estimation using spherical probes. J Microsc 206(Pt 1):54–64.

Nadler JV, Cotman CW, Lynch GS. 1973. Altered distribution of choline acetyltransferase and acetylcholinesterase activities in the developing rat dentate gyrus following entorhinal lesion. Brain Res 63:215–220.

Preuss TM, Goldman-Rakic PS. 1991. Myelo- and cytoarchitecture of the granular frontal cortex and surrounding regions in the strepsirhine primate Galago and the anthropoid primate Macaca. J Comp Neurol 310:429–474.

Raghanti MA, Simic G, Watson S, Stimpson CD, Hof PR, Sherwood CC. 2011. Comparative analysis of the nucleus basalis of Meynert among primates. J Neurosci 16:1–15.

Robertson RT, Mostamand F, Kageyama GH, Gallardo KA, Yu J. 1991. Primary auditory cortex in the rat: transient expression of acetylcholinesterase activity in developing geniculocortical projections. Brain Res Dev Brain Res 58: 81–95.

Ruediger T, Bolz J. 2007. Neurotransmitters and the development of neuronal circuits. Adv Exp Med Biol 621:104–105.

Sakai T, Hirata S, Fuwa K, Sugama K, Kusunoki K, Makishima H, Eguchi T, Yamada S, Ogihara N, Takeshita H. 2012. Fetal brain development in chimpanzees versus humans. Curr Biol 22:R791–791.

Sano M, Kaga K, Kuan CC, Ino K, Mima K. 2007. Early myelination patterns in the brainstem auditory nuclei and pathway: MRI evaluation study. Int J Pediatr Otorhinolaryngol 71:1105–1115.

Sano M, Kuan CC, Kaga K, Itoh K, Ino K, Mima K. 2008. Early myelination patterns in the central auditory pathway of the higher brain: MRI evaluation study. Int J Pediatr Otorhinolaryngol 72:1479–1486.

Semba K. 2004. Phylogenetic and ontogenetic aspects of the basal forebrain cholinergic neurons and their innervation of the cerebral cortex. Prog Brain Res 145:3–43.

Shaw P, Kabani NJ, Lerch JP, Eckstrand K, Lenroot R, Gogtay N, Greenstein D, Clasen L, Evans A, Rapoport JL, Giedd JN, Wise SP. 2008. Neurodevelopmental trajectories of the human cerebral cortex. J Neurosci 28:3586–3594.

Sherwood CC, Gordon AD, Allen JS, Phillips KA, Erwin JM, Hof PR, Hopkins WD. 2011. Aging of the cerebral cortex differs between humans and chimpanzees. Proc Natl Acad Sci U S A 108:13029–13034.

Shi Y, Short SJ, Knickmeyer RC, Wang J, Coe CL, Niethammer M, Gilmore JH, Zhu H, Styner MA. 2013. Diffusion tensor imaging-based characterization of brain neurodevelopment in primates. Cereb Cortex 23:36–48.

Shideler KK, Yan J. 2010. M1 muscarinic receptor for the development of auditory cortical function. Mol Brain 3:29.

Simons M, Trajkovic K. 2006. Neuron-glia communication in the control of oligodendrocyte function and myelin biogenesis. J Cell Sci 119(Pt 21):4381–4389.

Simons M, Trotter J. 2007. Wrapping it up: the cell biology of myelination. Curr Opin Neurobiol 17:533–540.

Sowell ER, Peterson BS, Thompson PM, Welcome SE, Henkenius AL, Toga AW. 2003. Mapping cortical change across the human life span. Nat Neurosci 6:309–315.

Stevens B, Porta S, Haak LL, Gallo V, Fields RD. 2002. Adenosine: a neuron-glial transmitter promoting myelination in the CNS in response to action potentials. Neuron 36: 855–868.

Takahashi E, Dai G, Rosen GD, Wang R, Ohki K, Folkerth RD, Galaburda AM, Wedeen VJ, Ellen Grant P. 2011. Developing neocortex organization and connectivity in cats revealed by direct correlation of diffusion tractography and histology. Cereb Cortex 21:200–211.

Wake H, Lee PR, Fields RD. 2011. Control of local protein synthesis and initial events in myelination by action potentials. Science 333:1647–1651.

Watson RE, Desesso JM, Hurtt ME, Cappon GD. 2006. Postnatal growth and morphological development of the brain: a species comparison. Birth Defects Res B Dev Reprod Toxicol 77:471–484.

Waxman SG. 1977. Conduction in myelinated, unmyelinated, and demyelinated fibers. Arch Neurol 34:585–589.

Yakovlev PL, Lecours AR. 1967. The myelogenetic cycles of regional maturation of the brain. In: Minkowski A, editor. Regional development of the brain in early life. Oxford, UK: Blackwell Publishers. p 3–70.

Zhang ZW. 2006. Canadian Association of Neurosciences review: postnatal development of the mammalian neocortex: role of activity revisited. Can J Neurol Sci 33:158–169.